blood®
Regular Article

TRANSPLANTATION

The OTUD1-Notch2-ICD axis orchestrates allogeneic T cell–mediated graft-versus-host disease

Qiao Cheng,[1,*] Dong Wang,[1,*] Xiaoxuan Lai,[1,*] Yin Liu,[1] Yibo Zuo,[2] Wenli Zhang,[1] Lei Lei,[1] Jia Chen,[1] Hong Liu,[1] Ying Wang,[1] Haiyan Liu,[3] Hui Zheng,[2] Depei Wu,[1] and Yang Xu[1]

[1]National Clinical Research Center for Hematologic Diseases, Jiangsu Institute of Hematology, The First Affiliated Hospital of Soochow University, Institute of Blood and Marrow Transplantation, Collaborative Innovation Center of Hematology and [2]Jiangsu Key Laboratory of Infection and Immunity, Institutes of Biology and Medical Sciences, Soochow University, Suzhou, China; and [3]Immunology Programme, Life Sciences Institute and Department of Microbiology and Immunology, Yong Loo Lin School of Medicine, National University of Singapore, Singapore

KEY POINTS

- **OTUD1 is a novel deubiquitinase of Notch2-ICD and promotes the severity of T cell–mediated aGVHD.**
- **The OTUD1/Notch2-ICD axis is a potential therapeutic target for alleviating aGVHD.**

Disorders of the ubiquitin-proteasome system (UPS) are known to influence the incidence and mortality of various diseases. It remains largely unknown whether and how the UPS affects the onset and progression of acute graft-verus-host disease (aGVHD) after allogeneic hematopoietic stem cell transplantation (allo-HSCT). This study demonstrated that the deubiquitinase OTUD1 is an essential regulator of aGVHD. Activation of CD4$^+$ T cells after allo-HSCT, elevated the protein levels of OTUD1, which in turn interacted with the Notch2-ICD (NICD) to cleave the ubiquitin of NICD at the K1770 site, thereby inducing NICD protein accumulations in T cells. OTUD1-driven NICD signaling promoted the differentiation and functions of Th1 and Th17 cells and amplified the cascade of aGVHD. Moreover, by screening a FDA-approved drugs library the study identified dapagliflozin as an inhibitor targeting the OTUD1/NICD axis. Dapagliflozin administration significantly prolonged the survival of aGVHD mice. This study characterized a previously unknown role of OTUD1 in T cell–mediated allogeneic responses and provided a promising therapeutic strategy to target OTUD1 for the alleviation of aGVHD.

Introduction

Although the methods of allogeneic hematopoietic stem cell transplantation (allo-HSCT) are constantly being optimized, acute graft-versus-host disease (aGVHD) remains the main cause of transplant–related morbidity and mortality.[1,2] Currently, aGVHD is characterized by an allogeneic response mediated by donor T cells, including uncontrolled T-cell activation and proliferation, and the release of proinflammatory cytokines.[3-5] However, intrinsic signaling activities in allogeneic T (allo-T) cells, which drive the pathological process of aGVHD, remain largely unknown.

Deubiquitinases (DUBs) have been recently shown to participate in the pathogenesis of diverse diseases, therefore, DUBs represent attractive and promising therapeutic targets.[6,7] However, the roles of DUBs in aGVHD after allo-HSCT have been rarely reported. OTUD1 is a member of the Ovarian Tumor (OTU) family and has been reported to regulate innate antiviral[8] and antifungal[9] immunity, as well as breast cancer metastasis[10] and carcinoma.[11] However, inhibitors of OTUD1 have not yet been developed, thus largely restricting the studies and clinical applications related to OTUD1.

Notch signaling is required for the development and function of lymphocytes.[12] RBPJ-dependent Notch signaling plays an indispensable role in the onset of T-cell differentiation in a prethymic niche.[13] Targeting Notch signaling by pan-Notch inhibitors can alleviate aGVHD; however, these treatments are associated with severe systemic side effects.[14] Targeting individual Notch receptors or ligands with antibodies or drugs is a promising strategy to prevent allograft rejection.[15,16] However, the specific role of Notch2-ICD (NICD) in aGVHD remains unknown. In addition, Notch2 ubiquitination can be regulated by SCF FBW7,[17] DTX3[18] and TRAF6[19]; however, a DUB of Notch2 has not been identified.

This study demonstrated that OTUD1 is a DUB of Notch2 that regulates ubiquitination of the NICD protein at the K1770 site and further promotes T-cell pathogenicity and aGVHD. Moreover, we identified dapagliflozin as an inhibitor targeting the OTUD1/NICD axis, which eventually inhibited T-cell activation and effector function and prolonged the survival of aGVHD mice.

Materials and methods

Patients and sample collection

The study includes the following 2 separate groups of patients: 154 patients who received HSCT in the First Affiliated Hospital of Soochow University from January 2015 to December 2018 (supplemental Table 1, available on the *Blood* website), and a

second group of 40 patients who received HSCT in the First Affiliated Hospital of Soochow University from June 2019 to February 2022 (supplemental Table 2). The clinical characteristics of these patients were shown in supplemental Tables 1 and 2. Informed consent was obtained from each patient and was approved by the Ethics Committee of Soochow University. All patients have completed clinical follow-up data. Peripheral blood samples were collected in patients before HSCT and from 28 to 100 days after HSCT. PBMCs were isolated from peripheral blood by Ficoll (Cytiva, Marlborough, NJ). Competitive risk analysis was used to calculate the cumulative incidence of II to IV aGVHD and a Gray test was used to compare the difference between 2 groups. Kaplan-Meier survival curve analysis was used to calculate the overall survival (OS) and a log-rank test was used to compare the differences between 2 groups.

Mice

Specific pathogen–free C57BL/6 ($H2K^b$) and BALB/c ($H2K^d$) mice (aged 6-8 weeks) were purchased from SLAC Laboratory Animal Center (Shanghai, China). OTUD1 knockout (KO) mice on C57BL/6 ($H2K^b$) background were kindly provided by Professor Hui Zheng, and all OTUD1-KO mice were validated by polymerase chain reaction with genomic DNA extracted from mouse tails according to the description given previously. All animals were raised in specific pathogen–free conditions and in accordance with the guidelines approved by the Institutional Laboratory Animal Care and Use Committee of Soochow University. Experiments have been approved by the ethics committee of the Soochow University.

Establishment of aGVHD mice

BALB/c recipient mice received total body irradiation of 650 cGy (2 doses of 375 cGy with 4-hour interval) by an RAD 320 X-ray Irradiator. Recipient mice were injected intravenously with 1×10^7 bone marrow (BM) cells or T cell–depleted BM cells and 5×10^6 splenocytes or sorted 2×10^6 splenic $CD4^+$ T cells isolated from C57BL/6 mice. Survivals were recorded every day. Body weight and aGVHD scores were evaluated and recorded every 2 days.

Statistical analysis

GraphPad Prism 8.0 was used for all the statistics calculation and figure production. Data comparisons were analyzed with Student *t* test. Spearman rank correlation analysis was used in correlation analysis. OS was analyzed by using the Kaplan–Meier methodology and comparisons were performed by using the log-rank test. A 2-tailed $P < .05$ was considered statistically significant.

Results

OTUD1 is upregulated in allo-T cells during allogeneic responses

To clarify whether ubiquitination is involved in the T cell-driven aGVHD, we established the syngeneic HSCT and allogeneic HSCT mouse models and then sorted syngeneic T (syn-T) cells and allo-T cells to analyze the transcriptome (Figure 1A; supplemental Figure 1A). The results of GO (gene ontology) analysis showed that the hydrolase activity and thiol-dependent DUB in allo-T cells were significantly changed compared with those in syn-T cells (supplemental Figure 1B-C). The levels of both USP and OTUD family members were changed in allo-T cells (Figure 1B). Given that the roles of the USP family members in T cells have been reported,[20-23] we further evaluated the expression of the OTUD family members in allo-T cells. The messenger RNA (mRNA) levels of *Otud1*, *Otud4 and Otud5* were significantly upregulated in allo-T cells (Figure 1C). Interestingly, the mRNA levels of both *Otud1* and *Otud5* were elevated in allogeneic $CD4^+$ T cells but not in allogeneic $CD8^+$ T cells (supplemental Figure 1D-F). OTUD1 protein levels increased consistently and significantly in $CD4^+$ T cells upon stimulation, but not in $CD8^+$ T cells (Figure 1D). Furthermore, we collected PBMCs from patients with non-GVHD and patients with aGVHD after allo-HSCT. The results showed that the mRNA levels of *Otud1* were markedly upregulated in PBMCs isolated from patients with aGVHD (Figure 1E-F). Furthermore, we sorted $CD3^+$ T cells from PBMCs of non-aGVHD and aGVHD patients and found that the mRNA levels of *Otud1* were significantly upregulated in $CD3^+$ T cells isolated from aGVHD patients (supplemental Figure 2A-B). Consistent with the results in mice, *Otud1* mRNA levels significantly increased in $CD4^+$ T but not $CD8^+$ T cells isolated from patients with aGVHD (supplemental Figure 2C-D). These results indicated that OTUD1 was abnormally upregulated in allo-T cells and $CD4^+$ T cells of patients with aGVHD.

OTUD1 levels are positively associated with the incidence and severity of aGVHD in patients who underwent allo-HSCT

To investigate the potential prognostic value of OTUD1 in patients with aGVHD after allo-HSCT, additional patient specimens were collected. Patients with grade 2-4 aGVHD expressed higher levels of *Otud1* in PBMCs when compared with patients with grade 0 to 1 aGVHD after HSCT (Figure 1F), and the receiver operating characteristic curve-based association was significant (Figure 1G). In addition, patients with $OTUD1^{hi}$ had a higher cumulative incidence of grade 2-4 aGVHD after allo-HSCT than that of patients with $OTUD1^{lo}$ (Figure 1H), and had a poor OS after allo-HSCT (Figure 1I). Thus, we believe that OTUD1 may be a potential biomarker for predicting the incidence and severity of aGVHD in patients with allo-HSCT and a potential therapeutic target of aGVHD.

OTUD1 regulates the activation, expansion, and allogeneic responses of $CD4^+$ T cells

Next, we sorted wild type (WT)-$CD4^+$ T and OTUD1-deficient $CD4^+$ T cells from WT and OTUD1-KO mice to perform proteomic analysis (supplemental Figure 3A-C). The results of GO analysis showed that the type I interferon signaling pathway, T-cell activation and inflammatory responses were significantly changed in OTUD1-deficient $CD4^+$ T cells (supplemental Figure 3D). OTUD1 has been reported to inhibit IFNβ production during RNA virus infection.[24] Here, in activated $CD4^+$ T cells, OTUD1 deficiency did not affect the production of IFNβ (supplemental Figure 3E).

To evaluate the role of OTUD1 in the regulation of inflammatory responses and T-cell activation, $CD4^+$ T and $CD8^+$ T cells isolated from OTUD1-deficient and WT mice were initially tested to assess the levels of the transcription factors T-bet (Th1), RORγt (Th17), and GATA3 (Th2). The data showed that OTUD1 deficiency dramatically inhibited T-bet, RORγt, and GATA3

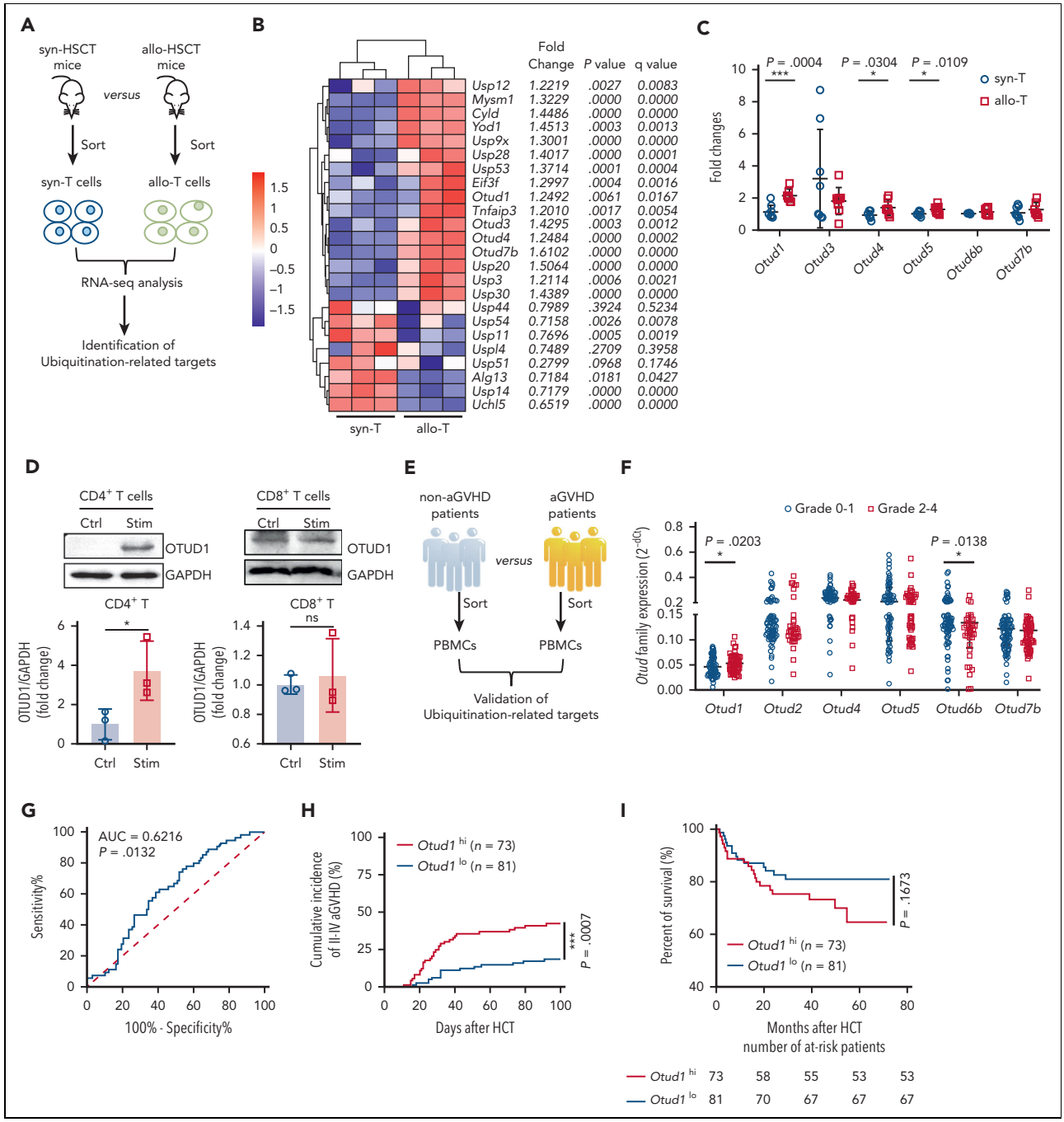

Figure 1. Allogeneic response-induced upregulation of OTUD1 exacerbates aGVHD progression in HCT patients. (A) A schematic diagram of the mice experiments. (B) Heat map showing the differential thiol-dependent deubiquitinating enzymes. (C) T cells were isolated from syn-HSCT (n = 8) and allo-HSCT mice (n = 8) and the mRNA levels of *Otud1*, *Otud3*, *Otud4*, *Otud5*, *Otud6b* and *Otud7b* were evaluated by reverse transcription quantitative polymerase chain reaction (RT-qPCR). (D) CD4$^+$ T cells and CD8$^+$ T cells purified from C57BL/6 mice were stimulated with anti-CD3 (2 μg/mL) and anti-CD28 (0.4 μg/mL) antibodies for 48 hours in vitro. Western blot was performed to evaluate the protein levels of OTUD1 in CD4$^+$ T and CD8$^+$ T cells with or without stimulation. (E) A schematic diagram of the patients experiments. (F) PBMCs were isolated from patients with aGVHD grade 0 to 1 (n = 109) and grade 2 to 4 (n = 57) and the mRNA levels of *Otud1*, *Otud2*, *Otud4*, *Otud5*, *Otud6b*, *Otud7b* were analyzed by RT-qPCR. (G) ROC curve for the *Otud1* mRNA level predicts aGVHD, cutoff value = 0.04633. (H) The cumulative incidence of II-IV aGVHD after HCT between *Otud1*^{hi} (>0.04633) and *Otud1*^{lo} (<0.04633) patients. (I) The OS of patients with *Otud1*^{hi} or *Otud1*^{lo} after HCT. The cumulative incidence of aGVHD and the survival curve were analyzed by log-rank (Mantel-Cox) test. Data in panels C,F are represented as mean ± standard deviation (SD); *P < .05, **P < .01, ***P < .001 (2-tailed unpaired Student t test). Data in panel D are representative of 3 independent experiments and are summarized as mean ± SD of 3 experiments. HCT, hematopoietic cell transplantation; ROC, receiver operating characteristic.

expression in activated CD4$^+$ T cells (Figure 2A) but not in activated CD8$^+$ T cells (Figure 2B). *Il2* and *Ifng* mRNA levels markedly decreased in OTUD1-deficient CD4$^+$ T cells stimulated with anti-CD3 and anti-CD28 antibodies (Figure 2C). Consistently, the protein levels of interleukin 2 (IL-2) and interferon gamma (IFN-γ) were dramatically reduced in activated OTUD1-deficient CD4$^+$ T cells according to the data of enzyme-linked immunosorbent assay (ELISA) (Figure 2D). However, *Ifng*,

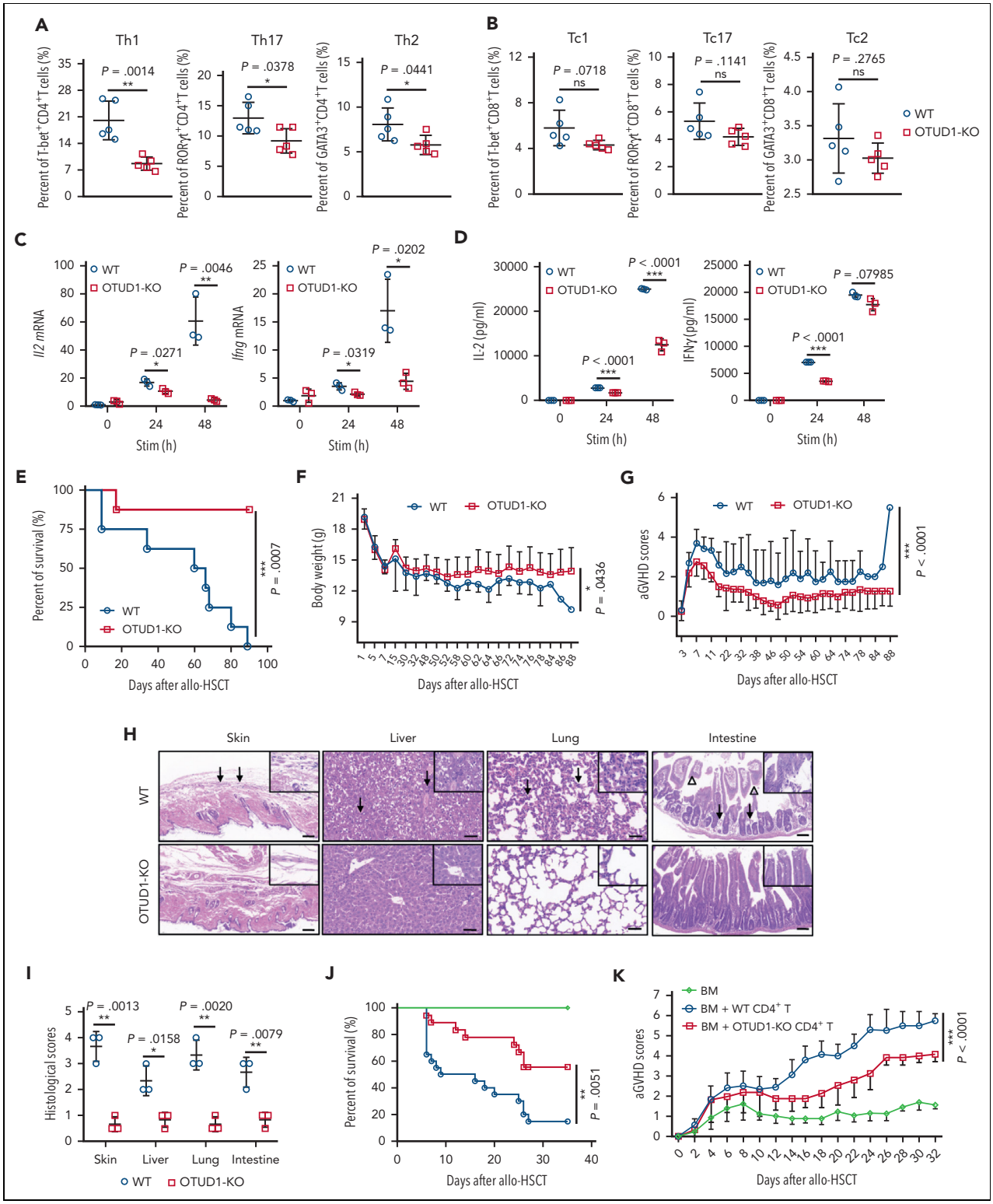

Figure 2. OTUD1 deficiency inhibits T-cell activation and proinflammatory cytokines production, alleviates aGVHD pathogenicity after allo-BMT (Bone Marrow Transplantation). (A-B) $CD4^+$ T cells (A) or $CD8^+$ T cells (B) isolated from C57BL/6 mice were stimulated with anti-CD3 (2 μg/mL) and anti-CD28 (0.4 μg/mL) antibodies for 48 hours, and were analyzed to detect the expression of T-bet, RORγt and Gata3 by flow cytometry. (C) Naive $CD4^+$ T cells purified from WT or OTUD1$^{-/-}$ mice on B6 background were stimulated with anti-CD3 (2 μg/mL) and anti-CD28 (0.4 μg/mL) antibodies for 24 or 48 hours. RT-qPCR was performed to evaluate the mRNA levels of IL-2 and IFN-γ. (D) Protein levels of IL-2 and IFN-γ were monitored by ELISA. (E-G) BM cells (1×10^7 per mouse) and splenocytes (5×10^6 per mouse) isolated from WT or OTUD1$^{-/-}$ mice on B6 background were transferred into lethally irradiated BALB/c mice ($n = 8$ for WT, $n = 8$ for OTUD1-KO). The survival (E) of aGVHD mice was observed twice daily, and body weight (F) and aGVHD scores (G) were observed and recorded every 2 days. (H) Representative images were shown in skin, liver, lung, and intestine of aGVHD mice by hematoxylin and eosin (HE) staining (scale bar, 100 μm; arrows, infiltrating lymphocytes; triangles, apoptotic epithelial cells). (I) Histological scores of skin, liver, lungs, and intestine of aGVHD mice were evaluated. (J-K) BM cells (1×10^7 per mouse) isolated from WT mice and $CD4^+$ T cells (2×10^6 per mouse) isolated from WT or OTUD1$^{-/-}$ mice were transferred into lethally irradiated BALB/c mice ($n = 13$ for BM, $n = 20$ for WT, $n = 18$ for OTUD1-KO). The survival of aGVHD mice was observed twice a day (J), aGVHD

Il2, *Il17a* and *Tnfa* mRNA levels were not significantly altered by OTUD1 deficiency in $CD8^+$ T cells (supplemental Figure 3F). These results indicated that OTUD1 deficiency significantly inhibits the functions of $CD4^+$ T cells but not $CD8^+$ T cells. Furthermore, OTUD1 deficiency decreased CD44 expression on $CD4^+$ T cells stimulated with anti-CD3 and anti-CD28 antibodies (supplemental Figure 4A). Subsequently, we found that the absence of OTUD1 significantly restrained the proliferation of $CD4^+$ T cells stimulated with anti-CD3 and anti-CD28 antibodies (supplemental Figure 4B). Overall, OTUD1 deficiency repressed the activation and proliferation of $CD4^+$ T cells in vitro.

To further test the effect of OTUD1 on the allo-responses of $CD4^+$ T cells, we transferred WT or OTUD1$^{-/-}$ $CD4^+$ T cells into lethally irradiated BALB/c mice and intraperitoneally injected EdU in the schematic diagram (supplemental Figure 4C). The proportion and number of donor-derived $CD4^+$ T cells significantly decreased (supplemental Figure 4D-E), indicating that OTUD1 depletion may impair the ability of donor $CD4^+$ T cells to proliferate. Consistent with the in vitro results, the proportion and number of EdU^+CD4^+ T cells were dramatically reduced in BALB/c mice receiving OTUD1$^{-/-}$$CD4^+$ T cells (supplemental Figure 4F-G). Meanwhile, the transfer of OTUD1$^{-/-}$ $CD4^+$ T cells into lethally irradiated BALB/c mice resulted in a lower production of IFN-γ (supplemental Figure 4H). Together, these results suggested that OTUD1 deficiency subverts the proliferation of $CD4^+$ T cells in vivo.

Elimination of donor OTUD1 alleviates the pathogenesis of aGVHD in mice

To explore whether OTUD1 plays an essential role in the development of aGVHD, WT or OTUD1-deficient BM cells and splenocytes were transferred into lethally irradiated BALB/c mice to establish the aGVHD models. Donor OTUD1 deficiency prolonged the survival of aGVHD mice (Figure 2E), ameliorated weight loss (Figure 2F), and decreased the aGVHD scores (Figure 2G). In addition, donor OTUD1 deficiency attenuated the pathogenesis of the target organs, including the skin, liver, lung and intestine (Figure 2H-I; supplemental Figure 4I). Interestingly, we further clarified that OTUD1 deficiency in donor $CD4^+$ T cells prolonged the survival of aGVHD mice (Figure 2J) and lowered aGVHD scores (Figure 2K). However, OTUD1 deficiency in donor $CD8^+$ T cells did not significantly affect the survival (supplemental Figure 4J) and aGVHD scores (supplemental Figure 4K) of aGVHD mice. Collectively, these findings suggested that OTUD1 deficiency in donor $CD4^+$ T but not $CD8^+$ T cells attenuates the severity of aGVHD.

OTUD1 deficiency alters T cell fate, inhibits Th1 and Th17 differentiation, and promotes Treg differentiation after allo-BMT

To further reveal how donor OTUD1 scarcity alleviates aGVHD, splenocytes from the recipients treated with WT or OTUD1-deficient BM cells and splenocytes were isolated to perform single-cell RNA sequencing (supplemental Figure 5A). Single-cell transcriptomes of splenocytes were analyzed, and 23 transcriptionally distinct cell clusters were identified (Figure 3A; supplemental Figure 5B). The proportion of $CD4^+$ T cells in total splenocytes did not change significantly (Figure 3B); however, the ratio of $CD4^+$ T cells/$CD8^+$ T cells decreased (Figure 3C). The results of gene set enrichment analysis (GSEA) of T cells revealed that OTUD1 deficiency negatively regulated the following KEGG (Kyoto Encylopaedia of Genes and Genomes) pathways: allograft rejection, antigen processing and presentation, the Toll-like receptor signaling pathway, and cytokine–cytokine receptor interactions (Figure 3D). Therefore, we reclustered T cells and identified 9 transcriptionally distinct T cell clusters, including proliferating T cells (MKi67^{hi}T), activated $CD3^+$ T cells (a$CD3^+$T), activated $CD4^+$ T cells (a$CD4^+$T), activated $CD8^+$ T cells (a$CD8^+$T), Th1 cells, and Tc1 cells (Figure 3E; supplemental Figure 5C). Interestingly, the proportion of Th1 ($CD4^+IFNγ^+$) cells decreased in the recipients receiving OTUD1-KO BM cells and splenocytes (Figure 3F), indicating that donor OTUD1 deficiency may inhibit Th1 differentiation. Furthermore, the results of monocle analysis implicated the start-to-end differentiation of T cells, and MKi67^{hi} T cells were identified as a starting point that differentiated into activated T cells, Th1 cells, and Tc1 cells (Figure 3G-H). The results of GSEA of MKi67^{hi} T cells revealed that OTUD1 deficiency negatively regulated the KEGG pathways, which positively regulated the inflammatory response (Figure 3I), and positively regulated the transforming growth factor β (TGF-β) signaling pathway (Figure 3J). Donor OTUD1 scarcity reduced the proportion of $CD69^+$ T cells (supplemental Figure 5D). Consistently, the proportions of $IFNγ^+CD4^+$ T cells (Th1), IL-$17A^+CD4^+$ T cells (Th17) (Figure 3K) and $IFNγ^+CD8^+$ T cells (Tc1), IL-$17A^+CD8^+$ T cells (Tc17) (supplemental Figure 5E) dramatically decreased when OTUD1 was deficient. In addition, the TGF-β signaling pathway is well known to be critical for Treg (regulatory T) differentiation. We demonstrated that the absence of OTUD1 promoted the differentiation of Treg cells (Figure 3L). In addition, serum tumor necrosis factor α and IL-6 were downregulated in OTUD1-deficient cells (supplemental Figure 5F). Furthermore, OTUD1 deficiency negatively regulated the T-cell receptor (TCR) signaling pathway and induced the downregulation of the key proteins in TCR signaling (supplemental Figure 5G-H). In summary, donor OTUD1 deficiency inhibits T-cell activation, differentiation, and proinflammatory cytokine production in aGVHD mice.

OTUD1 regulates Notch2 ubiquitination and degradation and positively correlates with Notch2 target genes

To investigate the molecular mechanism by which OTUD1 regulates T-cell pathogenicity, we firstly compared the total protein levels in activated OTUD1-deficient $CD4^+$ T cells with those in WT-$CD4^+$ T cells using proteomics analysis (supplemental Figure 3A-C). The results of KEGG enrichment analysis showed that OTUD1 deficiency altered Th1 and Th2 cell differentiation (Figure 4A). To identify the target substrates of OTUD1, we focused on the downregulated proteins and found that the levels of Notch2 and STAT1 decreased in activated OTUD1-deficient $CD4^+$ T cells to some extent (Figure 4B). However, the results of GSEA of activated $CD4^+$ T cells indicated that OTUD1 elimination negatively regulated JAK-STAT signaling and

Figure 2 (continued) scores were observed and recorded every 2 days (K). Log-rank (Mantel-Cox) test was used to analyze the survival curve. Data in panels A-D,I are represented as mean ± SD with biological replicates; $^*P < .05$, $^{**}P < .01$, $^{***}P < .001$ (two-tailed unpaired Student *t* test).

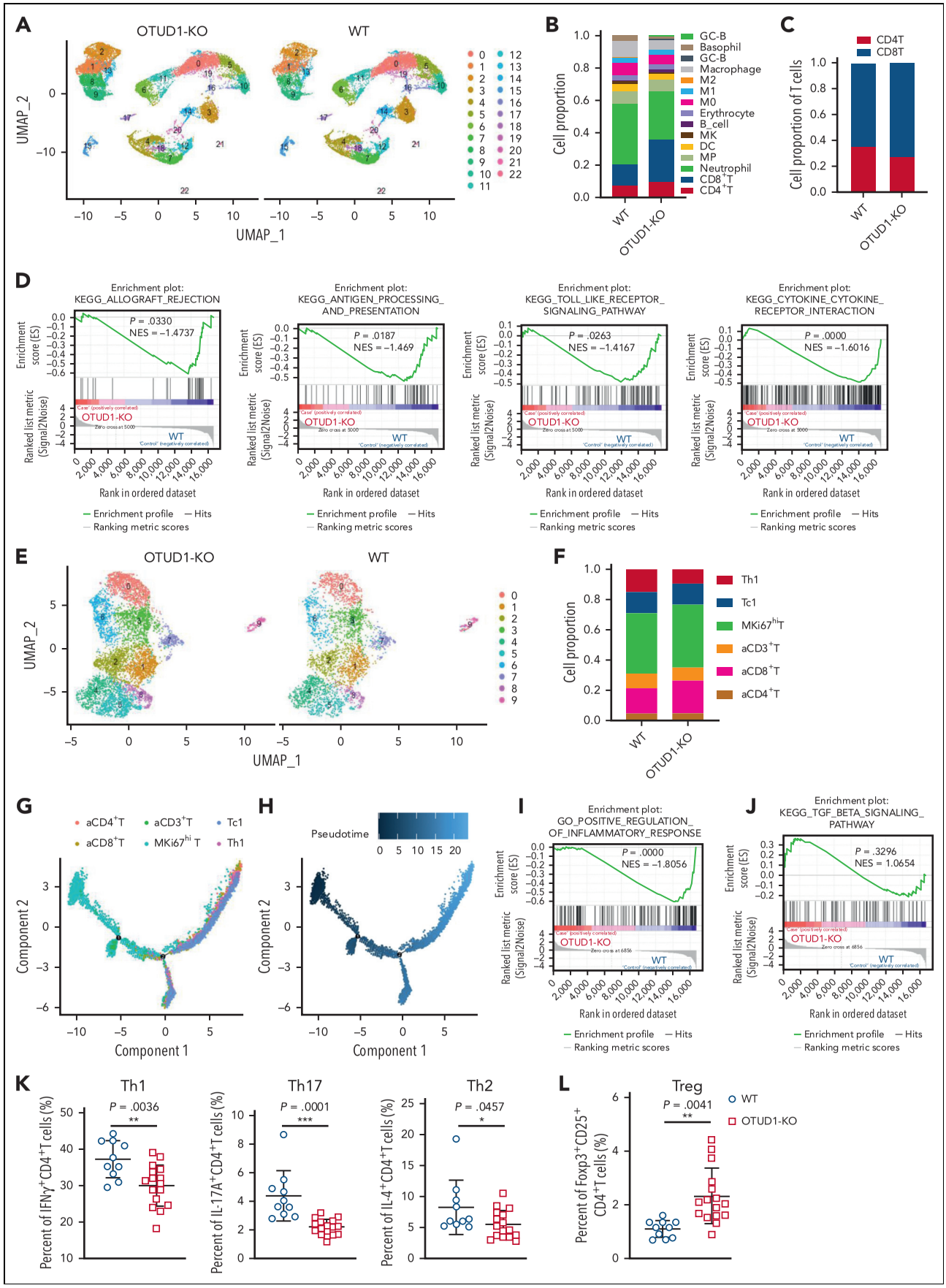

Figure 3.

downregulated STAT1 mRNA levels (Figure 4C). Therefore, we evaluated whether Notch2 is a novel OTUD1 substrate protein. We demonstrated that Notch2, but not Notch1, Notch3, or Notch4, was degraded in vitro in activated OTUD1-deficient $CD4^+$ T cells (Figure 4D; supplemental Figure 6A). Next, we assessed the impact of OTUD1 on Notch2 ubiquitination. The results showed that knockdown of OTUD1 dramatically increased the ubiquitination of Myc-Notch2 (Figure 4E; supplemental Figure 6B). Furthermore, to clarify whether OTUD1-regulated Notch2 ubiquitination depends on its DUB activity, we mutated the amino acids C320 and H431 into A320 and Q431 in OTUD1, respectively. We demonstrated that OTUD1 was able to deubiquitinate Notch2, whereas the OTUD1-AQ mutant did not influence Notch2 ubiquitination (Figure 4F). These data revealed that OTUD1 deubiquitinates Notch2 in a manner dependent on its deubiquitinating enzyme activity. Furthermore, we demonstrated that both OTUD1 and Notch2 protein levels were clearly upregulated in Jurkat cells and $CD4^+$ T cells upon activation (Figure 4G-H) but were not upregulated in $CD8^+$ T cells (supplemental Figure 6C). In addition, OTUD1 deficiency did not affect Notch2 protein levels in $CD8^+$ T cells upon activation (supplemental Figure 6D). Moreover, Notch2 target genes, including *Hes1*, *Hes5*, *Hey1* and *HeyL*, were all downregulated in activated OTUD1-deficient $CD4^+$ T cells (Figure 4I). Consistently, OTUD1 expression levels positively correlated with Notch2 target genes in patients who underwent hematopoietic cell transplantation (Figure 4J). Taken all together, these findings demonstrated that OTUD1 deficiency induces the degradation of Notch2 and inhibits Notch2 target genes.

OTUD1 interacts with NICD and cleaves ubiquitin from the K1770 site of the NICD protein

We then sought to investigate how OTUD1 regulates Notch2. The data indicated that OTUD1 colocalized with Notch2 (Figure 5A). Notch2 interacted with pCDH-OTUD1 in Jurkat cells (Figure 5B). Consistent with this finding, Notch2 interacted with OTUD1 in $CD4^+$ T cells (supplemental Figure 6E). These results suggested a mutual interaction between OTUD1 and Notch2. Furthermore, we investigated the association of OTUD1 with Notch2 in activated T cells. Interestingly, the activation of T cells promoted the OTUD1-Notch2 interaction (Figure 5C). Therefore, these findings suggested that OTUD1 interacts with Notch2 in resting T cells, and this association dramatically increases in T cells upon activation.

To determine which domain of Notch2 binds to OTUD1, we generated the following constructs: pCDH-Myc-Notch2-full length, pCDH-Myc-Notch2-ECD, pCDH-Myc-Notch2-TMD, and pCDH-Myc-NICD (Figure 5D). The results of confocal microscopy showed that OTUD1 colocalized with Myc-full length and Myc-NICD but not with Myc-Notch2-ECD and Myc-Notch2-TMD (Figure 5E). The data of immunoprecipitation indicated that OTUD1 interacted with Flag-NICD (Figure 5F). These results suggested that OTUD1 interacts with the intracellular domain of Notch2 (NICD). Moreover, the ubiquitination of Myc-NICD was enhanced when OTUD1 was knocked down (Figure 5G). The lysine (K) sites of NICD ubiquitination have been reported to include K1701, K1703, K1705, K1738, K1768, K1770, and K2121.[25-29] To determine which lysine sites of NICD were involved in the ubiquitination regulation by OTUD1, we constructed the K1701R, K1703R, K1705R, K1738R, K1768R, K1770R, and K2121R mutants of NICD (Figure 5H). We found that OTUD1 deubiquitinated only the K1770 site of NICD (Figure 5I). Consistently, we demonstrated that OTUD1 overexpression did not upregulate the protein levels of NICD-K1770R (Figure 5I). In summary, OTUD1 interacts with NICD and deubiquitinates NICD at the K1770 site.

NICD is essential for OTUD1–mediated T-cell pathogenicity and aGVHD progression

We then clarified the effect of inhibition of Notch signaling on T-cell activation, effector function and proliferation. The data showed that DAPT (GSI-IX), a γ-secretase inhibitor that is known to inhibit Notch signaling, markedly reduced the proportion of $CD69^+CD4^+$ T cells (supplemental Figure 7A), effector $CD4^+$ T cells ($CD44^+CD62L^-$), (supplemental Figure 7B), and $Ki67^+CD4^+$ T cells (supplemental Figure 7C), and downregulated the production of IFN-γ and IL-2 (Figure 6A). To further determine whether OTUD1 regulates T-cell activation and function through Notch2, we blocked Notch signaling with DAPT or knocked down Notch2 using short hairpin RNAs against Notch2. We noticed that OTUD1 was unable to activate TCR signal transduction when Notch2 was inhibited or knocked down (Figure 6B-C). Furthermore, NICD was overexpressed in aGVHD mice transferred with WT or OTUD1-KO BM cells and splenocytes (Figure 6D). The results showed that NICD overexpression augmented aGVHD-related mortality (Figure 6E), enhanced aGVHD scores (Figure 6F), and aggravated pathological damage to the target organs in aGVHD mice (Figure 6G-H). These results indicated that NICD aggravates the severity of aGVHD alleviated by OTUD1 deficiency in vivo. Thus, we demonstrated that NICD is essential for OTUD1 to regulate both TCR signal transduction in activated T cells and the development of aGVHD in mice.

Targeting the OTUD1/NICD axis with dapagliflozin restricts T-cell activation and effector function, attenuating the severity of aGVHD in mice

To identify potential inhibitors of OTUD1, we performed drug screening using computer-aided drug design technology. The

Figure 3. OTUD1 deficiency subverts T-cell fate, inhibits Th1 and Th17 differentiation, promotes Treg differentiation, and restricts proinflammatory factor secretion. (A) UMAP (uniform manifold approximation and projection) displays cell populations in the spleen of aGVHD mice receiving WT or OTUD1-deficient cells by sc-RNA sequencing (sc-RNA seq) (n = 2 for WT, n = 2 for OTUD1-KO). Cluster 1 (C1): $CD8^+$ T, C2: $CD4^+$ T, C8/C9: proliferating T ($MKi67^{hi}$ T), C6/C11/C0/C19/C5/C10: neutrophil, C16: megakaryocyte (MK), C4: MP, C18/C7: monocyte, C12: M1, C22: M2, C3: macrophage, C14/C20: DC, C15: basophil, C17: B cell, C21: GC-B cell, C13: erythrocyte. (B) Cell proportion of clusters in aGVHD mice receiving WT or OTUD1-deficient cells. (C) The proportion of $CD4^+$ T cells and $CD8^+$ T cells in T cells of aGVHD mice receiving WT or OTUD1-deficient cells are shown. (D) GSEA analysis of T-cell differential genes implicated by sc-RNA seq shows the KEGG signaling pathways. (E) UMAP displays cell populations of T-cell reclusters in aGVHD mice receiving WT or OTUD1-deficient cells by sc-RNA seq (C0/C3/C6/C9: proliferating T ($MKi67^{hi}$ T), C7/C8: activated $CD3^+$ T ($aCD3^+$ T), C5: activated $CD4^+$ T ($aCD4^+$ T) and activated $CD8^+$ T ($aCD8^+$ T), C2: $aCD8^+$ T, C4: helper $CD4^+$ T cell (Th1), C1: cytotoxic $CD8^+$ T cell (Tc1)). (F) Cell proportion of T-cell reclusters in aGVHD mice receiving WT or OTUD1-deficient cells. (G-H) Pseudotime analysis reveals the ordering of T-cell clusters along the pseudotime trajectory. (I-J) GSEA analysis showed inflammatory response (I) and TGF-β signaling pathway (J) enrichments of OTUD1-deficient T cells. (K-L) The percentage of Th1 ($IFNγ^+CD4^+$ T cells), Th17 ($IFNγ^+CD4^+$ T cells), Th2 ($IL\text{-}4^+CD4^+$ T cells) (K), and Treg ($CD25^+Foxp3^+CD4^+$ T cells) (L) in spleen of aGVHD mice receiving WT or OTUD1-deficient cells are analyzed by flow cytometry (n = 10 for WT, n = 16 for OTUD1-KO). Data in panels K-L are represented as mean ± SD; $^{**}P < .01$, $^{***}P < .001$ (2-tailed unpaired Student t test). DC, dendritic cell; MP, myeloid progenitors.

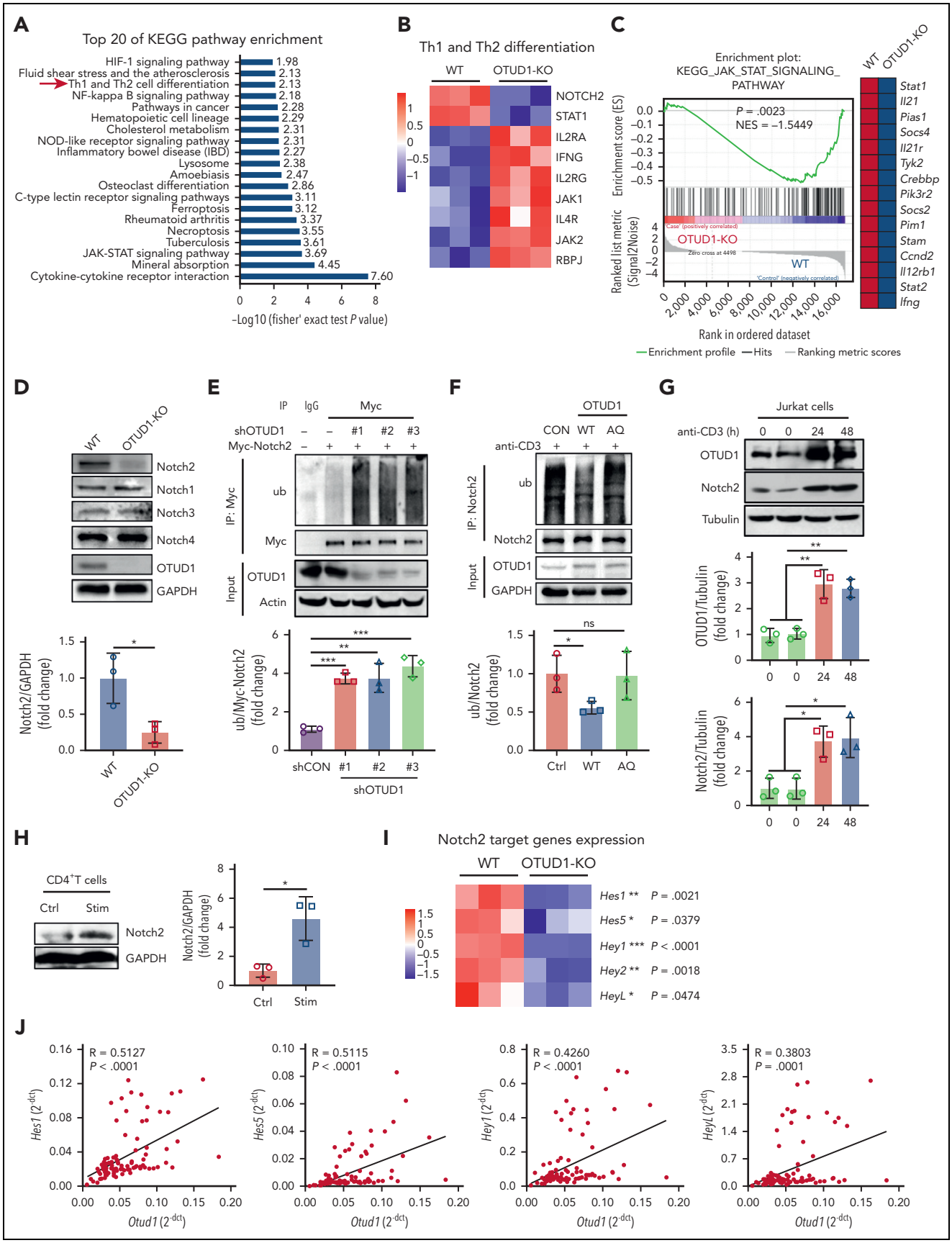

Figure 4.

key catalytic sites of OTUD1, including Asp317, Cys320, and His431, have been reported.[30] The 3D structure of the OTUD1 protein has been established (supplemental Figure 8A). The results of analysis of the 3D map provided by the SiteMap module of Schrödinger suite 2015 showed that the spatial positions of the amino acid residues of the catalytic triad of OTUD1 were located in a very close proximity to site 1 (white sphere) with high druggability (Figure 7A; supplemental Figure 8B). Furthermore, the fingerprints of the interactions between the US Food and Drug Administration–approved drugs and OTUD1 binding site 1 (supplemental Figure 8C) were used to screen for potential inhibitors targeting OTUD1 based on their docking scores. In addition, we screened various drugs that inhibited both NFAT activity measured by NFAT-luciferase assay (supplemental Figure 8D) and the activation of T cells in vitro (supplemental Figure 8E). Furthermore, we investigated the effects of potential inhibitors targeting OTUD1, which were initially identified by screening, on the protein levels of Flag-NICD. The results showed that empagliflozin, dapagliflozin, regorafenib, and dasatinib monohydrate significantly downregulated the protein levels of Flag-NICD (Figure 7B; supplemental Figure 8F). Interestingly, dapagliflozin treatment dramatically increased the ubiquitination of Flag-NICD (Figure 7C), indicating that dapagliflozin may be an efficient inhibitor of OTUD1. Both low and high doses of dapagliflozin induced considerable degradation of the Flag-NICD proteins (Figure 7D). Moreover, the molecular docking diagram of dapagliflozin and OTUD1 supported their association (Figure 7E). We demonstrated that dapagliflozin impaired the production of IFN-γ and IL-2 in $CD4^+$ T cells (Figure 7F). Dapagliflozin treatment significantly prolonged the survival of aGVHD mice (Figure 7G), decreased the aGVHD scores (Figure 7H), and attenuated the pathogenesis of the target organs, including the intestine, lung, liver, and skin (Figure 7I). Thus, we believe that dapagliflozin is a functional inhibitor targeting OTUD1 and is able to restrict T-cell activation and effector function to efficiently alleviate the severity of aGVHD in mice.

Discussion

This study demonstrated that targeting of DUB OTUD1 is a promising strategy to treat aGVHD. Thus, the study provides evidence supporting the feasibility of the design of the drugs that target the ubiquitin-proteasome system to prevent aGVHD.[31] Inhibition of the proteasome by bortezomib (an irreversible proteasome inhibitor) attenuates aGVHD by limiting the production of proinflammatory cytokines, suppressing T-cell proliferation and allogeneic responses[32] or impairing dendritic cell activation.[33] Therefore, proteasome inhibition is a potential treatment for aGVHD. However, both bortezomib and ixazomib treatments also have side effects, which increase the risk of infection, thrombocytopenia, cardiotoxicity, and neutropenia.[34] In a randomized BMTCTN clinical trial, bortezomib was reported to lack in clinical activity in limiting aGVHD.[35] There are limitations in translating findings from murine BMT models to human transplantation. In addition, distinct diseases may be associated with different characteristic alterations in the ubiquitin-proteasome system. Thus, different treatment schemes should be customized according to different characteristics.

Interestingly, the DUB OTUD1 is abnormally upregulated in allogeneic T cells. Currently, A20 is one of the few reported DUBs that influence GVHD.[36] However, the mRNA levels of A20 do not change significantly in allo-T cells, and the molecular mechanism by which A20 influences aGVHD remains unexplored. In addition, OTUD1 mRNA levels before allo-HSCT can be used to predict the cumulative incidence of aGVHD and OS of patients after HSCT. In the in vitro assay, OTUD1 protein levels were dramatically upregulated in $CD4^+$ T cells upon stimulation, but were not in $CD8^+$ T cells. Thus, targeting OTUD1 may be a potential strategy to hamper aGVHD while retaining GVL activity. OTUD1-deficient $CD4^+$ T cells lost the capacity to proliferate in vitro. The results of a mixed lymphocytes responses assay demonstrated that donor $CD4^+$ T cells did not proliferate in recipient mice in the absence of OTUD1. Moreover, in aGVHD mice, the lack of donor OTUD1 significantly prolonged the survival of recipient mice, and 9/10 mice survived over 100 days. These data suggested that the DUB OTUD1 may play a critical role in initiating the pathogenesis of aGVHD. Consistent with the in vitro data, donor OTUD1 deficiency impaired $CD4^+$ T-cell activation, effector function, and the secretion of inflammatory cytokines in aGVHD mice. Interestingly, the absence of donor OTUD1 also inhibited the activation and effector function of $CD8^+$ T cells. TGF-β signaling pathway is well known to be critical for Treg differentiation, and OTUD1 was reported to regulate SMAD7 stability, thereby inhibiting TGF-β signaling in breast cancer metastatic mice.[10] Interestingly, the results of GSEA of $MKi67^{hi}$ T cells revealed that OTUD1 deficiency positively regulated the TGF-β signaling pathway in aGVHD mice. We demonstrated that the absence of OTUD1 promotes the differentiation of Treg cells, indicating that the changes in $CD8^+$ T cells may be influenced by Treg cells in aGVHD mice.

Notch signaling plays a critical role in the initiation and development of aGVHD, and targeting individual Notch receptors or

Figure 4. OTUD1 absence destabilizes Notch2 and restrains the Notch2 signaling in activated $CD4^+$ T cells. (A) Top 20 of KEGG pathway enriched for OTUD1-deficient $CD4^+$ T cells stimulated with anti-CD3 (2 μg/mL) and anti-CD28 (0.4 μg/mL) antibodies compared with WT $CD4^+$ T cells by the proteomics. (B) Heat map presenting the differential proteins that affect Th1 and Th17 differentiation according to KEGG analysis. (C) GSEA analysis of T-cell differential genes in OTUD1-deficient $CD4^+$ T of aGVHD mice compared with WT $CD4^+$ T cells shows JAK-STAT signaling pathway by sc-RNA seq. (D) $CD4^+$ T cells isolated from WT or $OTUD1^{-/-}$ mice on B6 background were incubated with anti-CD3 (2 μg/mL) and anti-CD28 (0.4 μg/mL) antibodies and the protein levels of Notch2, Notch1, Notch3 and Notch4 were evaluated by western blot. (E) HEK293T cells were transfected with Myc-Notch2, control short hairpin RNA (shRNA) (shCON) or OTUD1shRNA (shOTUD1) plasmids. Myc-Notch2 proteins were immunoprecipitated with anti-Myc beads and the ubiquitination levels of Notch2 were evaluated by western blot. (F) Jurkat E6.1 cells were transfected with OTUD1-WT or OTUD1-AQ plasmids and incubated with anti-CD3 (0.1 μg/mL) antibodies and Notch2 proteins were immunoprecipitated with anti-Notch2 antibodies, the ubiquitination of Notch2 were analyzed by western blot. (G) Jurkat E6.1 cells were stimulated with anti-CD3 antibody (0.1 μg/mL) for 24 or 48 hours in vitro and the protein levels of OTUD1 and Notch2 were then assessed by western blot. (H) $CD4^+$ T cells isolated from C57BL/6 mice were stimulated with anti-CD3 (2 μg/mL) and anti-CD28 (0.4 μg/mL) antibodies and the protein levels of Notch2 were evaluated by western blot. (I) $CD4^+$ T cells isolated from WT or $OTUD1^{-/-}$ mice were stimulated with anti-CD3 (2 μg/mL) and anti-CD28 (0.4 μg/mL) antibodies for 24 hours and then the mRNA levels of *Hes1*, *Hes5*, *Hey1* and *HeyL* were by RT-qPCR. (J) The mRNA levels of *Hes1*, *Hes5*, *Hey1* and *HeyL* in PBMCs isolated from HCT patients (n = 104) were analyzed by RT-qPCR, the correlation between OTUD1 expression level and *Hes1*, *Hes5*, *Hey1* and *HeyL* expression levels was analyzed. Data in panel I are represented as mean ± SD; $^*P < .05$, $^{**}P < .01$, $^{***}P < .001$ (2-tailed unpaired Student t test). Data in panels D-H are representative of 3 independent experiments and are summarized as mean ± SD of 3 experiments. HCT, hematopoietic cell transplantation.

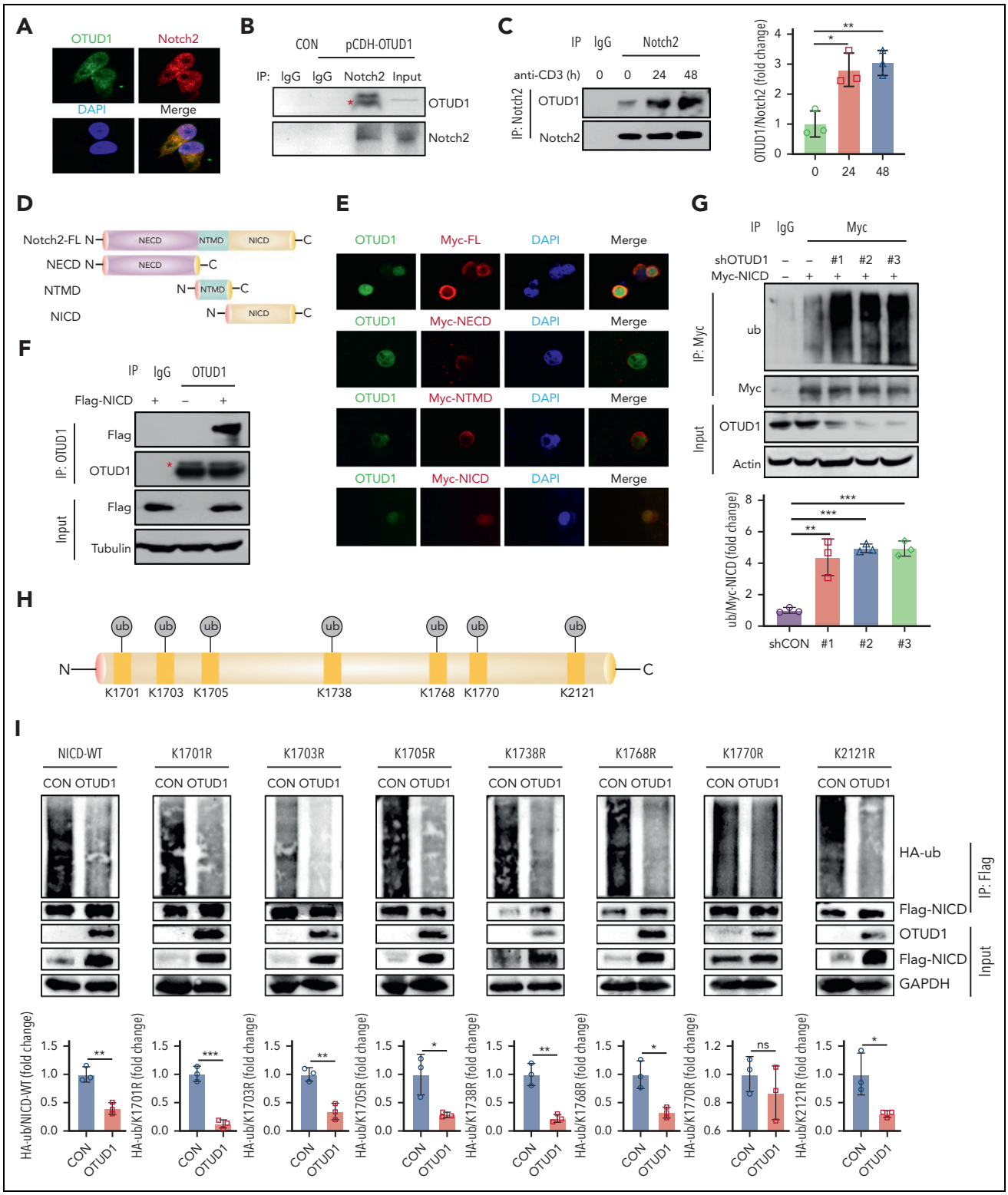

Figure 5. OTUD1 interacts with NICD and cleaves ubiquitin from the K1770 site of NICD. (A) Confocal microscopy was used to analyze colocalization between OTUD1 and Notch2. (B) Jurkat E6.1 cells were transfected with pCDH-OTUD1 plasmids. Notch2 proteins were immunoprecipitated with an anti-Notch2 antibody and then OTUD1 and Notch2 protein levels were analyzed by western blot. (C) Jurkat E6.1 cells were stimulated with anti-CD3 (0.1 μg/mL) antibody for 24 or 48 hours in vitro. Notch2 proteins were immunoprecipitated with anti-Notch2 antibody and then OTUD1 and Notch2 were assessed by western blot. (D) Schematic diagrams of Notch2 full-length and Notch2 different mutants. (E) HEK293T cells were transfected with Myc-Notch2-FL, Myc-Notch2-ECD, Myc-Notch2-TMD and Myc- NICD. The colocalization between Notch2 and OTUD1 were evaluated by confocal. (F) HEK293T cells were transfected with Flag-NICD. OTUD1 proteins were immunoprecipitated with an anti-OTUD1 antibody and then OTUD1 and Flag-NICD were analyzed by western blot. (G) HEK293T cells were transfected with Myc-NICD, shCON or shOTUD1. Myc-NICD proteins were immunoprecipitated with anti-Myc beads and the ubiquitination levels of NICD were evaluated by western blot. (H) Schematic diagram of the ubiquitination K site of NICD protein. (I) HEK293T cells were transfected with Flag-NICD-WT, K1701R, K1703R, K1705R, K1738R, K1768R, K1770R, K2121R, together with pCDH-OTUD1 and HA-ub. Flag-NICD proteins were analyzed by immunoprecipitation and immunoblotting. Data in panels B-C,F-G,I are representative of 3 independent experiments and data in panels C,G,I are summarized as mean ± SD of 3 experiments. FL, full length.

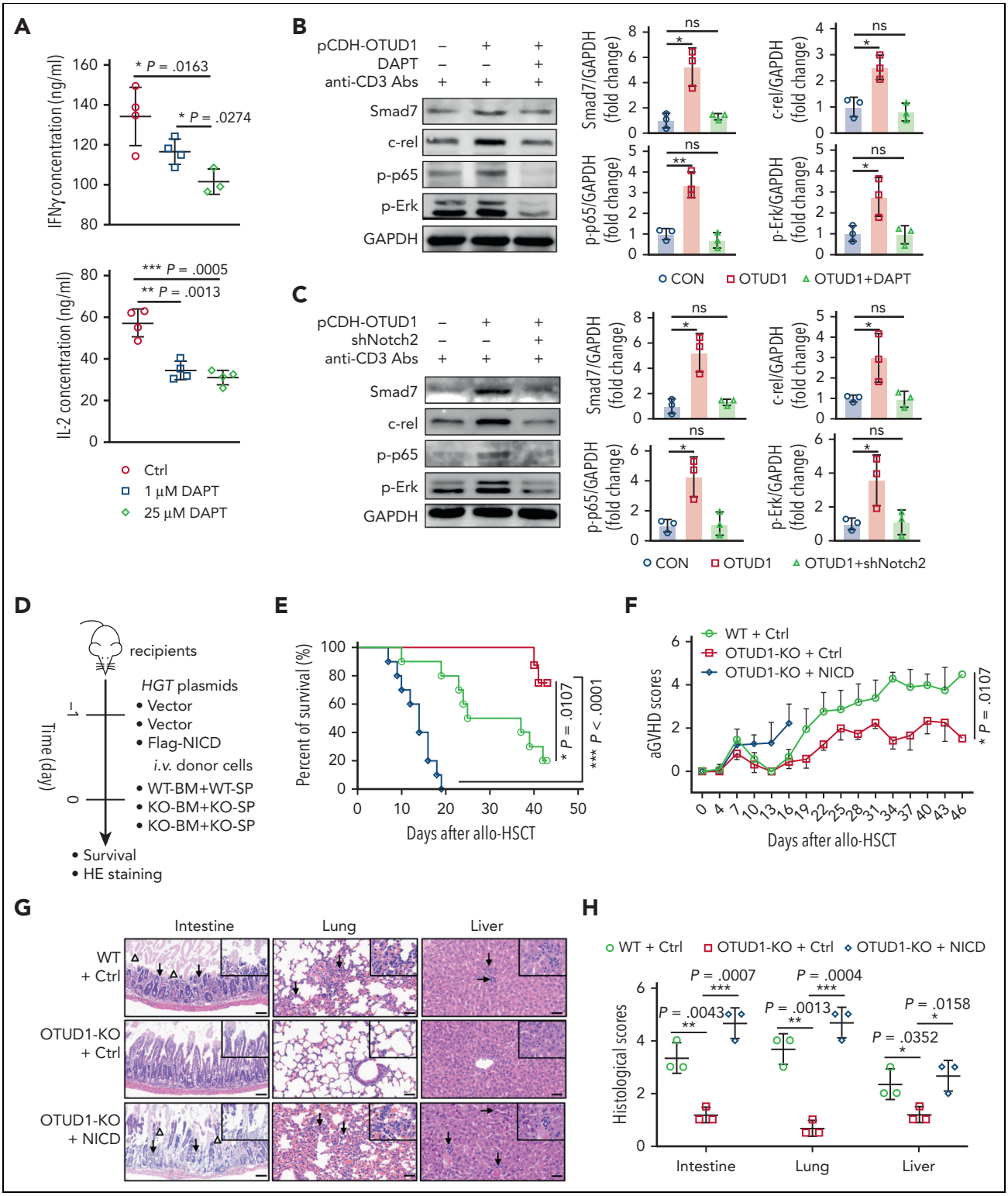

Figure 6. NICD is essential for OTUD1-mediated TCR signaling transduction that accelerates aGVHD progression. (A) $CD4^+$ T cells isolated from C57BL/6 mice were stimulated with anti-CD3 (2 μg/mL) and anti-CD28 (0.4 μg/mL) antibodies and incubated with control (Ctrl) or DAPT (1, 25 μM) for 24 hours in vitro, and then the protein levels of IFN-γ and IL-2 were monitored by ELISA. (B) Jurkat E6.1 cells stably expressing OTUD1 were incubated with anti-CD3 (0.1 μg/mL) antibody and with or without DAPT (5 μM) for 48 hours, and then Smad7, c-rel, p-p65 and p-Erk were assessed by western blot. (C) Jurkat E6.1 cells transfected with pCDH-OTUD1, shCON or Notch2 shRNA (shNotch2) plasmids were stimulated with anti-CD3 (0.1 μg/mL) antibody for 48 hours, and then Smad7, c-rel, p-LCK, p-p65, p-Erk and NFAT were monitored by western blot. (D) A schematic diagram of the mice experiments. (E-F) BM cells (1×10^7 per mouse) and splenocytes (5×10^6 per mouse) isolated from WT or OTUD1$^{-/-}$ mice on B6 background were transferred into lethally irradiated BALB/c mice injected with 80 μg Flag-NICD or Ctrl plasmids ($n = 10$ for WT + Ctrl group, $n = 8$ for OTUD1-KO + Ctrl group, $n = 10$ for OTUD1-KO + NICD group). The survival of aGVHD mice was observed twice 1 day (E), and the aGVHD scores were observed and recorded every 2 days (F). (G) Representative images of intestine, lung and liver of aGVHD mice by HE staining (scale bar, 100 μm; arrows, infiltrating lymphocytes; triangles, apoptotic epithelial cells). (H) Histological scores of intestine, lungs, and liver of aGVHD mice were evaluated. Log-rank (Mantel-Cox) test was used to analyze the survival curve. Data in panels A,H are represented as mean ± SD; $^*P < .05$, $^{**}P < .01$, $^{***}P < .001$ (2-tailed unpaired Student t test). Data in panels B,C are representative of 3 independent experiments and are summarized as mean ± SD of 3 experiments.

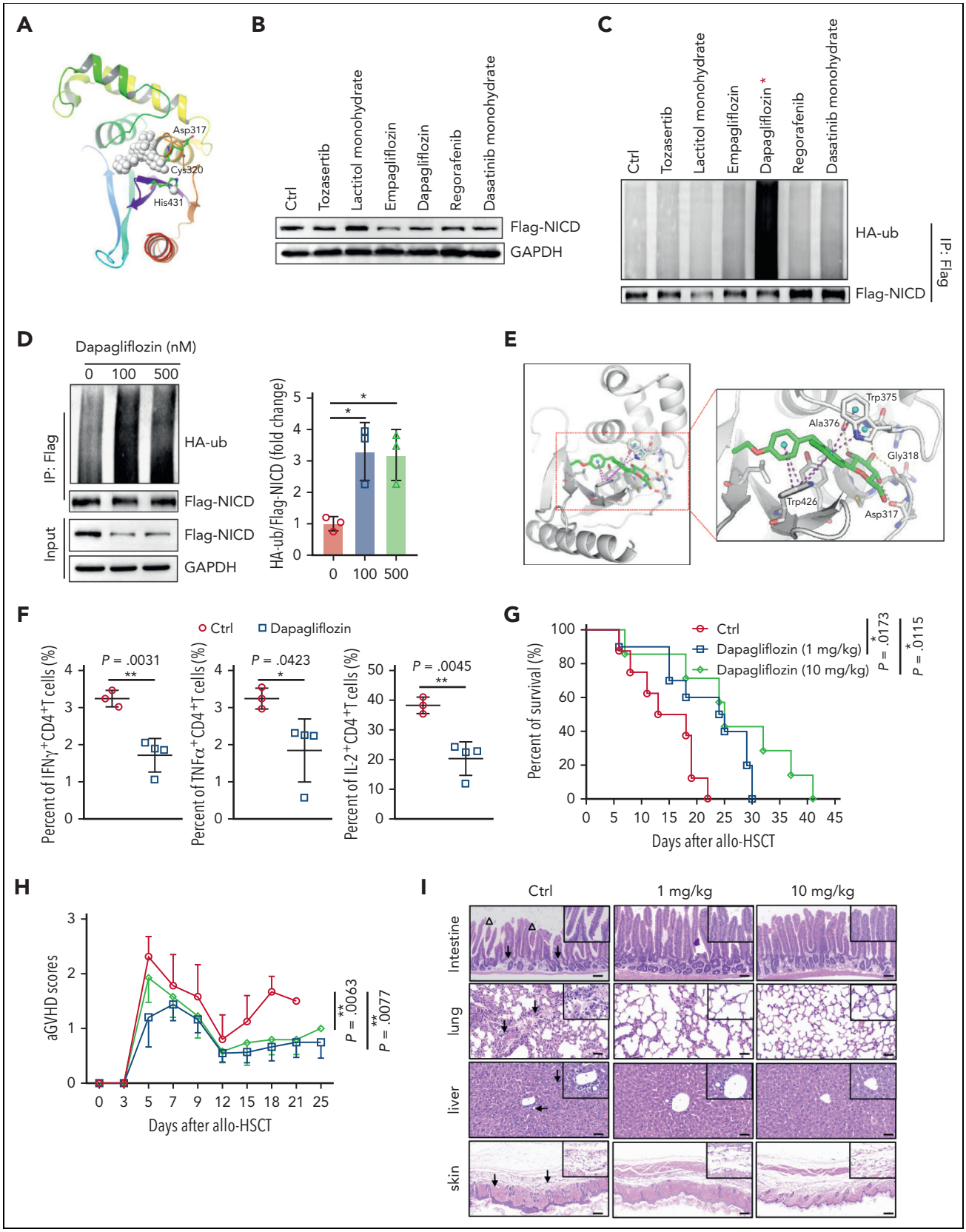

Figure 7. Targeting OTUD1/NICD axis by dapagliflozin impairs T-cell pathogenicity and attenuates the severity of aGVHD mice. (A) 3D map showing the spatial positions of the amino acid residues of the catalytic triad of OTUD1 and the site (white sphere) with high druggability predicted by the Sitemap. (B) HEK293T cells transfected with Flag-NICD, HA-ub, pCDH-OTUD1 plasmids were incubated with potential drugs (100 nM) as indicated for 24 hours, and then the protein levels of Flag-NICD were evaluated by western blot. (C) HEK293T cells transfected with Flag-NICD, HA-ub, pCDH-OTUD1 plasmids were incubated with potential drugs (100 nM) as indicated for 24 hours, and then Flag-NICD proteins were immunoprecipitated with anti-Flag beads and the ubiquitination of Flag-NICD was analyzed by western blot. (D) HEK293T cells

ligands effectively attenuates side effects caused by pan-Notch inhibitors.[14-16] NICD was expressed at a high level in Paneth cells after irradiation.[24] Consistently, Notch2 was expressed at a high level in $CD4^+$ T cells but not in $CD8^+$ T cells. The interaction of OTUD1 and Notch2 increased in T cells upon activation. OTUD1 was able to release ubiquitin from Notch2 and stabilize the Notch2 protein. Furthermore, OTUD1 interacted with the intracellular domain Notch2 (NICD) and regulated the ubiquitination of NICD. We demonstrated that OTUD1 mainly regulated the ubiquitin moiety at the K1770 site of the NICD protein. Moreover, OTUD1 overexpression activated TCR–mediated signal transduction, which was dependent on NICD, and NICD overexpression rescued the attenuation of aGVHD in mice receiving OTUD1-deficient cells.

The key catalytic sites of OTUD1 include Asp317, Cys320 and His431.[30] Thus, based on these catalytic sites, we screened potential drugs from the US Food and Drugs Administration–approved drug library based on their binding to the catalytic sites of OTUD1. Interestingly, dapagliflozin was identified as a potential drug inhibitor targeting OTUD1. Dapagliflozin treatment increased the ubiquitination of NICD, thus leading to the degradation of the NICD proteins. In addition, dapagliflozin treatment inhibited T-cell activation and the production of proinflammatory cytokines. Furthermore, administration of dapagliflozin dramatically prolonged the survival of aGVHD mice. As a selective SGLT2 inhibitor, dapagliflozin is a potent agent for treatment of type 1 and type 2 diabetes,[37,38] and stage 4 chronic kidney disease,[39] and has been shown to significantly attenuate heart failure.[40,41] The adverse events of dapagliflozin treatment were similar to those observed in the placebo group.[40] In aGVHD mice, the recipients treated with 10 mg/kg dapagliflozin survived longer than mice treated with 1 mg/kg dapagliflozin, with no apparent cytotoxicity or side effects.

Targeting DUBs is a promising strategy to prevent aGVHD. Over 100 deubiquitinating enzymes have been identified in mammals. Approximately 61 small molecule inhibitors of deubiquitinating enzymes have been reported, corresponding to 29 different DUBs,[42] which account for only ~30% of all mammalian DUBs, indicating potential availability of many undiscovered drugs that target the deubiquitinating enzymes. In summary, the data of the present study contribute to further understanding of the pathogenesis of aGVHD and provide new insight into future aGVHD treatments.

Acknowledgments

The authors thank Yuting Ma for extensive result discussion, and Jianhong Chu for his kind gifts of plasmids. All the human samples were from Jiangsu Biobank of Clinical Resources. The authors thank Qing Li and Qiao Du from CapitalBio Technology for the service of single-cell RNA sequence analysis, Qidong Zu from Oebiotech for the service of RNA sequence analysis, and Guannan Wang from PTM BioLab for the service of iTRAQ/TMT Proteome Quantitative Analysis. The authors are grateful to Renxiao Wang's group at the School of Pharmacy, Fudan University, for their technical aid in the virtual screening job described in this work. The authors thank Bo Hu, Dandan Lin, Tingting Zhu, and Xiaoqi Wang for their assistance in reviewing the manuscript.

This work was supported by the National Key R&D Program of China (2022YFC2502700), the National Natural Science Foundation of China (81800176, 82270222, 82020108003, 82070187, 81670164, 81730003), the Natural Science Foundation of Jiangsu Province (BK20180200), the National Key R&D Program of China (2019YFC0840604), and Priority Academic Program Development of Jiangsu Higher Education Institutions (PAPD).

Authorship

Contribution: Q.C. and Y.X. designed and performed the experiments; Q.C. prepared the figures and wrote the manuscript; D.W. performed the experiments and wrote part of the manuscript; X.L. contributed to collecting and testing human samples, and the breeding of OTUD1-KO mice; Y.L., W.Z., L.L., and Y.W. contributed to the experiments in vivo; Y.Z. contributed to the in vivo deubiquitination experiments and western blot; J.C. and H.L. contributed to providing the human specimens; H.L. contributed to designing experiments and discussing results; H.Z. provided OTUD1-KO mice, designed the experiments and wrote the manuscript; and Y.X., D.W., and H.Z. supervised the work.

Conflict-of-interest disclosure: The authors declare no competing financial interests.

ORCID profiles: Y.L., 0000-0002-9760-4227; Y.W., 0000-0002-8015-3546; H.Z., 0000-0002-4325-4946; D.W., 0000-0002-6312-3863.

Correspondence: Yang Xu, The First Affiliated Hospital of Soochow University, Soochow University, Suzhou 215123, China; email: yangxu@suda.edu.cn; Depei Wu, The First Affiliated Hospital of Soochow University, Soochow University, Suzhou 215123, China; email: drwudepei@163.com; and Hui Zheng, Institutes of Biology and Medical Sciences, Soochow University, Suzhou 215123, China; email: huizheng@suda.edu.cn.

Footnotes

Submitted 26 May 2022; accepted 6 December 2022; prepublished online on *Blood* First Edition 27 December 2022. https://doi.org/10.1182/blood.2022017201.

*Q.C., D.W., and X.L. contributed equally to this study.

Presented in abstract form at IMMUNOLOGY2020, the annual meeting of the American Association of Immunologists, Inc (AAI) on 19 May 2020.

Raw and processed RNA sequencing and single-cell RNA sequencing data have been shared in the Gene Expression Omnibus (GEO) database (accession numbers GSE212129, GSE212135, GSE212137, and GSE212162). Raw and processed proteomics data have been shared in the PRIDE database (project accession: PXD036217, username: reviewer_pxd036217@ebi.ac.uk, password: eHhdTDvG). FACS data have been

Figure 7 (continued) transfected with Flag-NICD, HA-ub, pCDH-OTUD1 plasmids were incubated with or without dapagliflozin (100, 500 nM) for 24 hours, and then the protein level of Flag-NICD were analyzed by western blot. (E) Molecular docking diagram of dapagliflozin and OTUD1. Green represents the compound dapagliflozin, purple dashed lines represent π-π interactions, yellow dashed lines represent hydrogen bonds, and proteins are shown in white cartoons. (F) $CD4^+$ T cells isolated from C57BL/6 mice were incubated with anti-CD3 (2 μg/mL) and anti-CD28 (0.4 μg/mL) antibodies and incubated with or without dapagliflozin (5 μM), and then the expression of IFN-γ and IL-2 were analyzed by flow cytometry. (G-I) BM cells (1×10^7 per mouse) and splenocytes (5×10^6 per mouse) isolated from C57BL/6 mice were transferred into lethally irradiated BALB/c mice intraperitoneally injected with Ctrl ($n = 8$), 1 mg/kg ($n = 10$) or 10 mg/kg ($n = 7$) dapagliflozin from day 1 to day 10 after transplantation. The survival (G) of aGVHD mice was observed twice 1 day, and aGVHD scores (H) were observed and recorded every 2 days. (I) Representative images were shown in intestine, lung, liver and skin of aGVHD mice by HE staining (scale bar, 100 μm; arrows, infiltrating lymphocytes; triangles, apoptotic epithelial cells). Log-rank (Mantel-Cox) test was used to analyze the survival curve (G). Data in panel F are represented as mean ± SD; $^*P < .05$, $^{**}P < .01$ (2-tailed unpaired Student *t* test). Data in panels B-D are representative of 3 independent experiments and data in panel D are summarized as mean ± SD of 3 experiments.

shared in the FlowRepository database and can be accessed via the following URLs: http://flowrepository.org/id/RvFrNr2bCvKPLlDSxlCcfi7kHWfWCgpScxqyZr6yGXKeCZFzCkRg5o5SUME4VfUG; http://flowrepository.org/id/RvFryqWREsVg8nfdXX3A3JgfPXP44M9Lgxzyc9AWzltCdrwGsxapPWsfL39mCalL; http://flowrepository.org/id/RvFramSxpRalUzmuH6Z7zi1nizD5zgdDKNsXdH4BqnNJjorIq1LWbFzpAAdkOamX; http://flowrepository.org/id/RvFr1QJ44LEw3PEioENvbk54fBRxElGSlKNqG2FSGMhm7SUG8tbzyPbrNribbNHH; http://flowrepository.org/id/RvFrMyekTA2D2WlMiY20odcv7yiuXEtXrYWfVRzebwPH3xKnRpeBY3XCCujG8dxK; http://flowrepository.org/id/RvFruojMYGl7v8xse48rGTyX99sBWsJU25dX51Zsy3t43r8nbOS61BRdsYpXC7kN; http://flowrepository.org/id/RvFrLdymTd9LsRzro8zYjQkhLvU97SzVv1dai6iH1Myzgb3no55EsDuBm9Ecy268; http://flowrepository.org/id/RvFrGEpLsYgsbVYmL1Ll1OCasbeXslAYQp60DlS54hNZ7JRtBzswzVio3hF4YZGV; http://flowrepository.org/id/RvFrMpX12b87llrVfMP6apAo7MZ5G3DqhRS8kKZsuJHK56yHaXuV2G4PhhtprQk9; and http://flowrepository.org/id/RvFrwsxWCXsJ1Liv6Ljw0hyjZKdkFQaF1WY9NzEkSmDHU72WYv9LmGdxP8Vquc1i.

All data generated or analyzed during this study are included in Figures 1–7 and supplemental Figures 1–9. All source data of western blots were included in supplemental Figure 9. Differentially expressed genes of allo-CD3$^+$ T vs syn-CD3$^+$ T cells, allo-CD4$^+$ T vs syn-CD4$^+$ T cells, allo-CD8$^+$ T vs syn-CD8$^+$ T cells were included in supplemental Table 3. Differentially expressed genes of clusters (cluster 0-22) were included in supplemental Table 4. Data are available upon request from the corresponding authors, Yang Xu (yangxu@suda.edu.cn), Depei Wu (drwudepei@163.com), and Hui Zheng (huizheng@suda.edu.cn).

The online version of this article contains a data supplement.

There is a *Blood* Commentary on this article in this issue.

The publication costs of this article were defrayed in part by page charge payment. Therefore, and solely to indicate this fact, this article is hereby marked "advertisement" in accordance with 18 USC section 1734.

REFERENCES

1. Blazar BR, Hill GR, Murphy WJ. Dissecting the biology of allogeneic HSCT to enhance the GvT effect whilst minimizing GvHD. *Nat Rev Clin Oncol*. 2020;17(8):475-492.
2. Zeiser R, Teshima T. Nonclassical manifestations of acute GVHD. *Blood*. 2021;138(22):2165-2172.
3. Voermans C, Hazenberg MD. Cellular therapies for graft-versus-host disease: a tale of tissue repair and tolerance. *Blood*. 2020;136(4):410-417.
4. Zeiser R. Advances in understanding the pathogenesis of graft-versus-host disease. *Br J Haematol*. 2019;187(5):563-572.
5. Zeiser R, Blazar BR. Acute graft-versus-host disease - biologic process, prevention, and therapy. *N Engl J Med*. 2017;377(22):2167-2179.
6. Harrigan JA, Jacq X, Martin NM, Jackson SP. Deubiquitylating enzymes and drug discovery: emerging opportunities. *Nat Rev Drug Discov*. 2018;17(1):57-78.
7. Clague MJ, Urbe S, Komander D. Breaking the chains: deubiquitylating enzyme specificity begets function. *Nat Rev Mol Cell Biol*. 2019;20(6):338-352.
8. Zhang L, Liu J, Qian L, et al. Induction of OTUD1 by RNA viruses potently inhibits innate immune responses by promoting degradation of the MAVS/TRAF3/TRAF6 signalosome. *PLoS Pathog*. 2018;14(5):e1007067.
9. Chen X, Zhang H, Wang X, et al. OTUD1 regulates antifungal innate immunity through deubiquitination of CARD9. *J Immunol*. 2021;206(8):1832-1843.
10. Zhang Z, Fan Y, Xie F, et al. Breast cancer metastasis suppressor OTUD1 deubiquitinates SMAD7. *Nat Commun*. 2017;8(1):2116.
11. Luo Q, Wu X, Zhao P, et al. OTUD1 activates caspase-independent and caspase-dependent apoptosis by promoting AIF nuclear translocation and MCL1 degradation. *Adv Sci (Weinh)*. 2021;8(8):2002874.
12. Radtke F, Wilson A, Mancini SJ, MacDonald HR. Notch regulation of lymphocyte development and function. *Nat Immunol*. 2004;5(3):247-253.
13. Chen ELY, Thompson PK, Zuniga-Pflucker JC. RBPJ-dependent Notch signaling initiates the T cell program in a subset of thymus-seeding progenitors. *Nat Immunol*. 2019;20(11):1456-1468.
14. Zhang Y, Sandy AR, Wang J, et al. Notch signaling is a critical regulator of allogeneic CD4+ T-cell responses mediating graft-versus-host disease. *Blood*. 2011;117(1):299-308.
15. Tran IT, Sandy AR, Carulli AJ, et al. Blockade of individual Notch ligands and receptors controls graft-versus-host disease. *J Clin Invest*. 2013;123(4):1590-1604.
16. Radojcic V, Paz K, Chung J, et al. Notch signaling mediated by Delta-like ligands 1 and 4 controls the pathogenesis of chronic GVHD in mice. *Blood*. 2018;132(20):2188-2200.
17. Fukushima H, Shimizu K, Watahiki A, et al. NOTCH2 Hajdu-Cheney mutations escape SCF(FBW7)-dependent proteolysis to promote osteoporosis. *Mol Cell*. 2017;68(4):645-658.e645.
18. Ding XY, Hu HY, Huang KN, et al. Ubiquitination of NOTCH2 by DTX3 suppresses the proliferation and migration of human esophageal carcinoma. *Cancer Sci*. 2020;111(2):489-501.
19. Zou Y, Yang R, Huang ML, et al. NOTCH2 negatively regulates metastasis and epithelial-mesenchymal transition via TRAF6/AKT in nasopharyngeal carcinoma. *J Exp Clin Cancer Res*. 2019;38(1):456.
20. Yang J, Wei P, Barbi J, et al. The deubiquitinase USP44 promotes Treg function during inflammation by preventing FOXP3 degradation. *EMBO Rep*. 2020;21(9):e50308.
21. Zou Q, Jin J, Hu H, et al. USP15 stabilizes MDM2 to mediate cancer-cell survival and inhibit antitumor T cell responses. *Nat Immunol*. 2014;15(6):562-570.
22. van Loosdregt J, Fleskens V, Fu J, et al. Stabilization of the transcription factor Foxp3 by the deubiquitinase USP7 increases Treg-cell-suppressive capacity. *Immunity*. 2013;39(2):259-271.
23. Jahan AS, Lestra M, Swee LK, et al. Usp12 stabilizes the T-cell receptor complex at the cell surface during signaling. *Proc Natl Acad Sci U S A*. 2016;113(6):E705-E714.
24. Yu S, Tong K, Zhao Y, et al. Paneth cell multipotency induced by Notch activation following injury. *Cell Stem Cell*. 2018;23(1):46-59.e45.
25. Beltrao P, Albanese V, Kenner LR, et al. Systematic functional prioritization of protein posttranslational modifications. *Cell*. 2012;150(2):413-425.
26. Akimov V, Barrio-Hernandez I, Hansen SVF, et al. UbiSite approach for comprehensive mapping of lysine and N-terminal ubiquitination sites. *Nat Struct Mol Biol*. 2018;25(7):631-640.
27. Povlsen LK, Beli P, Wagner SA, et al. Systems-wide analysis of ubiquitylation dynamics reveals a key role for PAF15 ubiquitylation in DNA-damage bypass. *Nat Cell Biol*. 2012;14(10):1089-1098.
28. Stukalov A, Girault V, Grass V, et al. Multilevel proteomics reveals host perturbations by SARS-CoV-2 and SARS-CoV. *Nature*. 2021;594(7862):246-252.
29. Zhang H, Zheng H, Zhu J, et al. Ubiquitin-modified proteome of SARS-CoV-2-infected host cells reveals insights into virus-host interaction and pathogenesis. *J Proteome Res*. 2021;20(5):2224-2239.
30. Mevissen TE, Hospenthal MK, Geurink PP, et al. OTU deubiquitinases reveal mechanisms of linkage specificity and enable ubiquitin chain restriction analysis. *Cell*. 2013;154(1):169-184.
31. Kasikis S, Etra A, Levine JE. Current and emerging targeted therapies for acute graft-versus-host disease. *BioDrugs*. 2021;35(1):19-33.
32. Kim Y, Yoo JY, Lee TJ, et al. Complex role of NK cells in regulation of oncolytic virus-bortezomib therapy. *Proc Natl Acad Sci U S A*. 2018;115(19):4927-4932.
33. Al-Homsi AS, Feng Y, Duffner U, et al. Bortezomib for the prevention and treatment

of graft-versus-host disease after allogeneic hematopoietic stem cell transplantation. *Exp Hematol*. 2016;44(9):771-777.

34. Schlafer D, Shah KS, Panjic EH, Lonial S. Safety of proteasome inhibitors for treatment of multiple myeloma. *Expert Opin Drug Saf*. 2017;16(2):167-183.

35. Bolaños-Meade J, Reshef R, Fraser R, et al. Three prophylaxis regimens (tacrolimus, mycophenolate mofetil, and cyclophosphamide; tacrolimus, methotrexate, and bortezomib; or tacrolimus, methotrexate, and maraviroc) versus tacrolimus and methotrexate for prevention of graft-versus-host disease with haemopoietic cell transplantation with reduced-intensity conditioning: a randomised phase 2 trial with a non-randomised contemporaneous control group (BMT CTN 1203). *Lancet Haematol*. 2019;6(3):e132-e143.

36. Fischer JC, Otten V, Steiger K, et al. A20 deletion in T cells modulates acute graft-versus-host disease in mice. *Eur J Immunol*. 2017;47(11):1982-1988.

37. Paik J, Blair HA. Dapagliflozin: a review in type 1 diabetes. *Drugs*. 2019;79(17):1877-1884.

38. Dhillon S. Dapagliflozin: a review in type 2 diabetes. *Drugs*. 2019;79(10):1135-1146.

39. Chertow GM, Vart P, Jongs N, et al. Effects of dapagliflozin in stage 4 chronic kidney disease. *J Am Soc Nephrol*. 2021;32(9):2352-2361.

40. Nassif ME, Windsor SL, Borlaug BA, et al. The SGLT2 inhibitor dapagliflozin in heart failure with preserved ejection fraction: a multicenter randomized trial. *Nat Med*. 2021;27(11):1954-1960.

41. Dewan P, Docherty KF, Bengtsson O, et al. Effects of dapagliflozin in heart failure with reduced ejection fraction and chronic obstructive pulmonary disease: an analysis of DAPA-HF. *Eur J Heart Fail*. 2021;23(4):632-643.

42. Schauer NJ, Magin RS, Liu X, Doherty LM, Buhrlage SJ. Advances in discovering deubiquitinating enzyme (DUB) inhibitors. *J Med Chem*. 2020;63(6):2731-2750.